Supporting Information

Langereis et al. 10.1073/pnas.0904266106

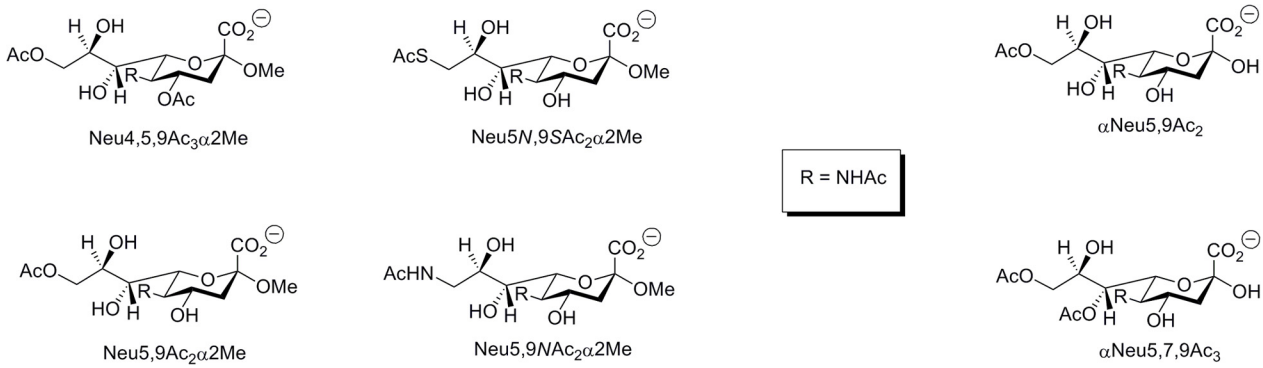

Fig. S1. Chemical structures of αNeu5,9Ac$_2$, αNeu5,7,9Ac$_3$ and synthetic HE receptor analogs.

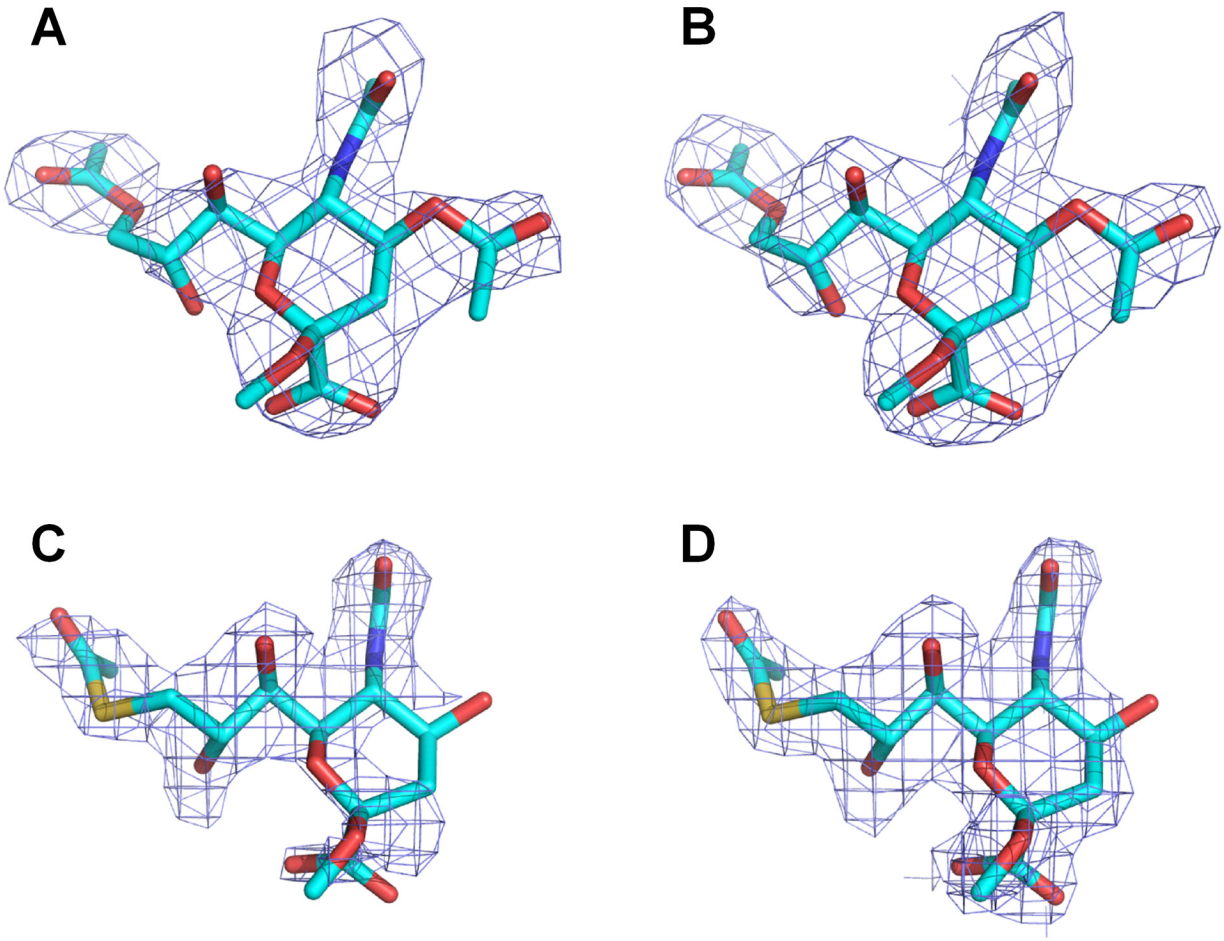

Fig. S2. Electron densities of receptor analogs. (*A*) PToV HE: difference electron density map calculated from the final model from which the ligand had been omitted. The contour level is 3.0σ. (*B*) PToV HE: 2Fo-Fc map of the final model contoured at the 1.0σ level. (*C*) BToV HE: difference electron density map calculated from the final model from which the ligand had been omitted. The contour level is 2.5σ. (*D*) BToV HE: 2Fo-Fc map of the final model contoured at the 1.0σ level. In BToV HE density for the ligand was observed at the receptor binding site in only one of 4 HE molecules present in the asymmetric unit: 2 sites were blocked by crystal contacts, whereas electron density in the aforementioned flexible monomer could not be interpreted.

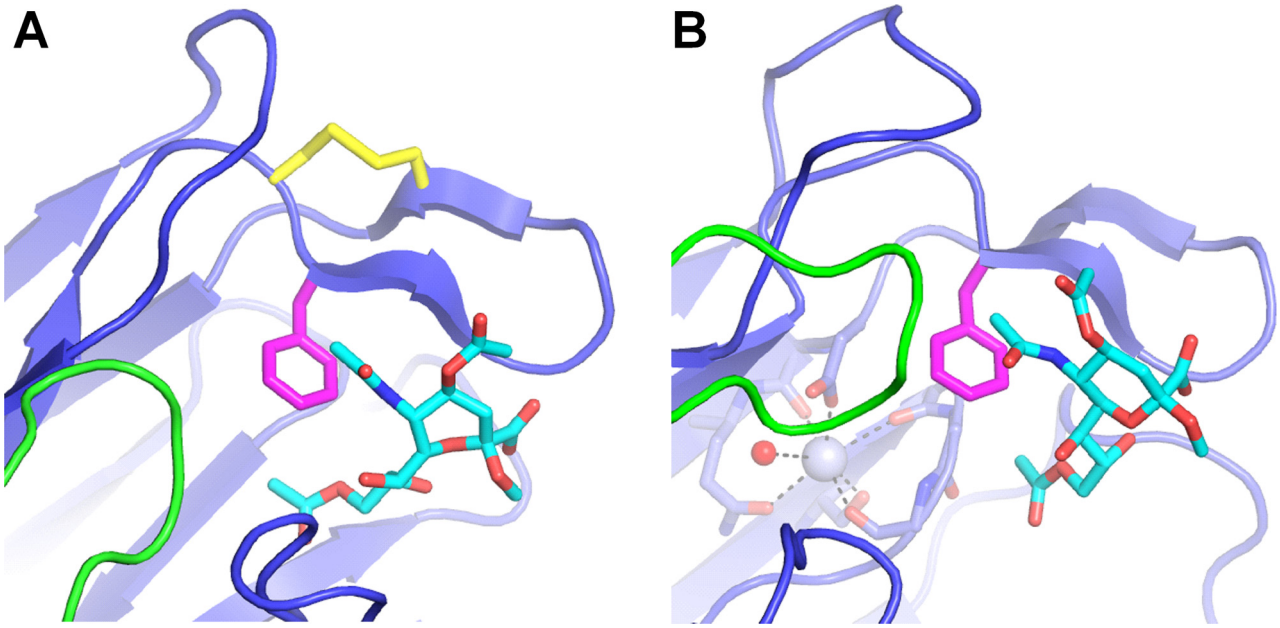

Fig. S3. Common and unique features of ToV and CoV HE receptor-binding sites. Ribbon diagrams are shown of the receptor-binding sites of (*A*) PToV HE and (*B*) BCoV HE (R domain, blue; E domain, green) with bound Neu4,5,9Ac$_3\alpha$2Me shown in stick representation (carbon, cyan; nitrogen, blue; oxygen, red). Shown in magenta is a common and essential phenylalanine located in a β-hairpin that is stabilized by a disulfide bridge (yellow sticks) in ToV HEs. In CoV HEs a metal-binding site stabilizes the receptor-binding site (potassium ion, gray sphere; water, red sphere; bonds to metal ion, black dashed lines). Proteins are depicted in orientations that were aligned by superposition of their conserved phenylalanine.

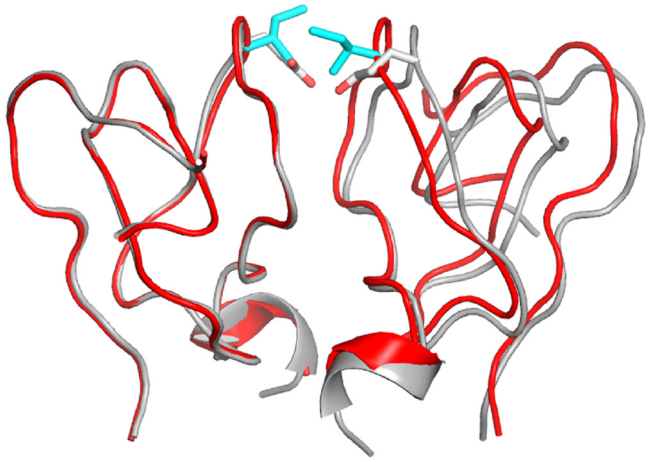

Fig. S4. The CR2 dimer interface in BToV HE is destabilized by Glu^{365}. Superposition of MP domain dimers of PToV HE (red) and BToV HE (gray) reveal a larger distance between the MP domains in BToV HE. Because of this ≈1.3-Å distance increase, the amount of buried surface area in BToV HE is ≈500 $Å^2$ less than in PToV HE (Table 2). We attribute the destabilization of the BToV HE dimer interface to Glu^{365}, whose negative charge is buried in the dimer interface, without charge compensation. In PToV HE an isoleucine is present at this position. Interestingly, the 4 BToV HE monomers in the asymmetric unit of the crystal display considerable mobility, which confirms that the dimer interface does not provide a stable link between monomers. TLS analysis [Schomaker V, Trueblood KN (1998) Correlation of internal torsional motion with overall molecular motion in crystals. *Acta Crystallogr B Structural Science* 54:507–514] suggests that monomer C, the more mobile one, undergoes a rigid body rotation with a mean square displacement of ≈1.7° around an axis approximately parallel to the 2-fold dimer axis. Because the position of Glu^{365} is occupied by a neutral amino acid in all other HEs, reduced dimer stability is likely a unique property of the HE of BToV strain Breda.

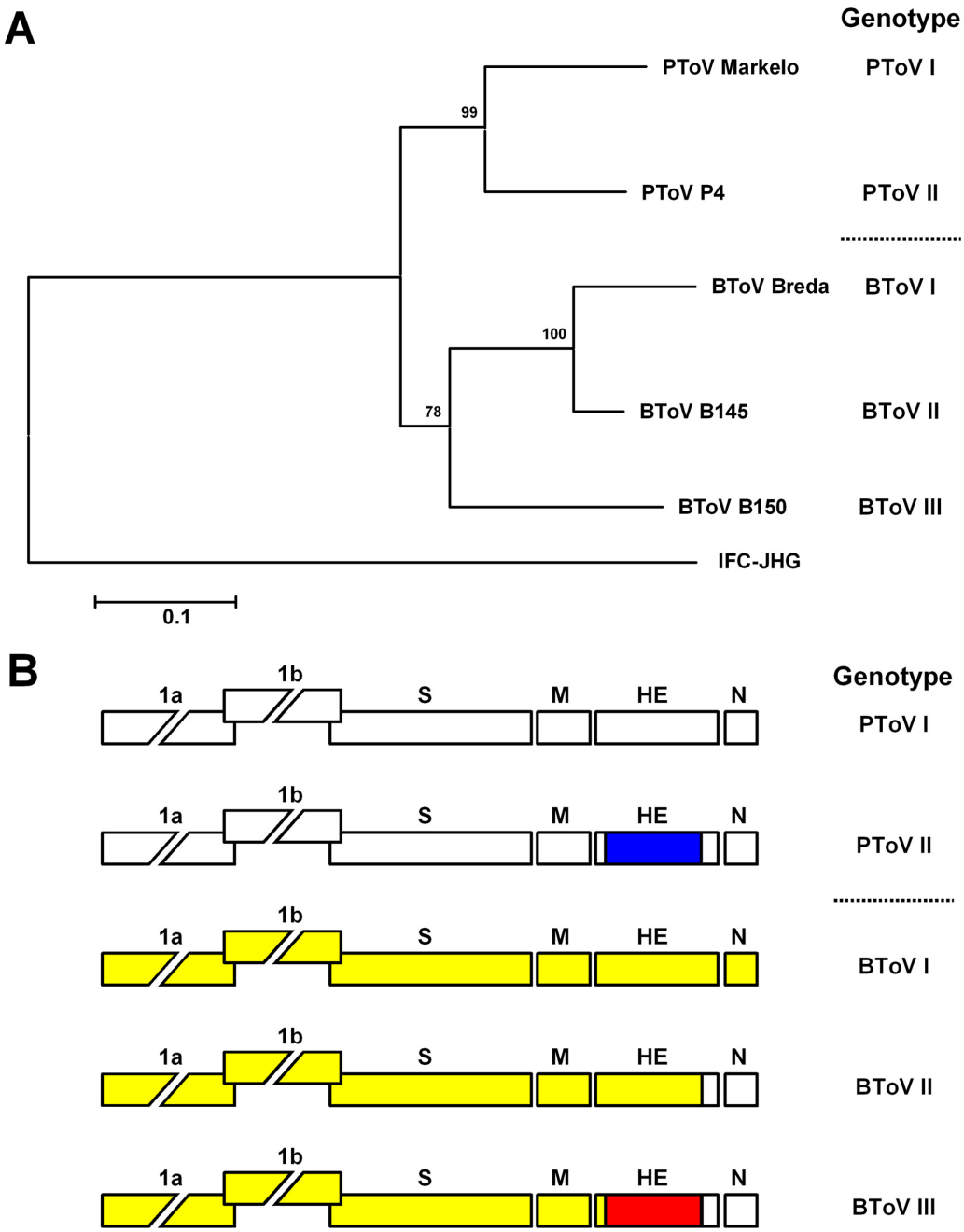

Fig. S5. Relationships between different torovirus genotypes and their HEs. (*A*) Rooted neighbor-joining tree depicting the relationships among HE genes of porcine torovirus genotypes I and II (represented by PToV strains Markelo and P4, respectively) and those of bovine torovirus genotypes I, II, and III (represented by BToV strains Breda, B145, and B150, respectively). The tree was constructed with the Kimura 2-parameter method and with the influenza C HEF gene as root. Confidence values calculated by bootstrap analysis (1,000 replicates) are shown at major branching points. Branch lengths are drawn to scale; the scale bar represents 0.1 nucleotide substitution per site. (*B*) Schematic representations of the genome organizations of the different torovirus genotypes. The genes for the replicase polyproteins (1a, 1b) and for the structural proteins S, M, HE, and N are depicted as boxes. Porcine torovirus types I and II share ≈95% sequence identity in the M and N genes, but only ≈77% in the coding sequences for the HE ectodomain (indicated by blue shading). The coding sequences for the HE ectodomains of type I and II BToV strains share ≈90% identity versus ≈70% identity with those of BToV type III strains (indicated by red shading). The differences between the torovirus genotypes apparently have arisen from homologous RNA recombination events during which PToV and BToV strains acquired new HE sequences from as yet unidentified toroviruses. For a detailed description of the phylogenetic and evolutionary relationships among torovirus field strains, please see ref. [Smits SL, et al. (2005) Nidovirus sialate-*O*-acetylesterases: Evolution and substrate specificity of coronaviral and toroviral receptor-destroying enzymes. *J Biol Chem* 280:6933–6941].

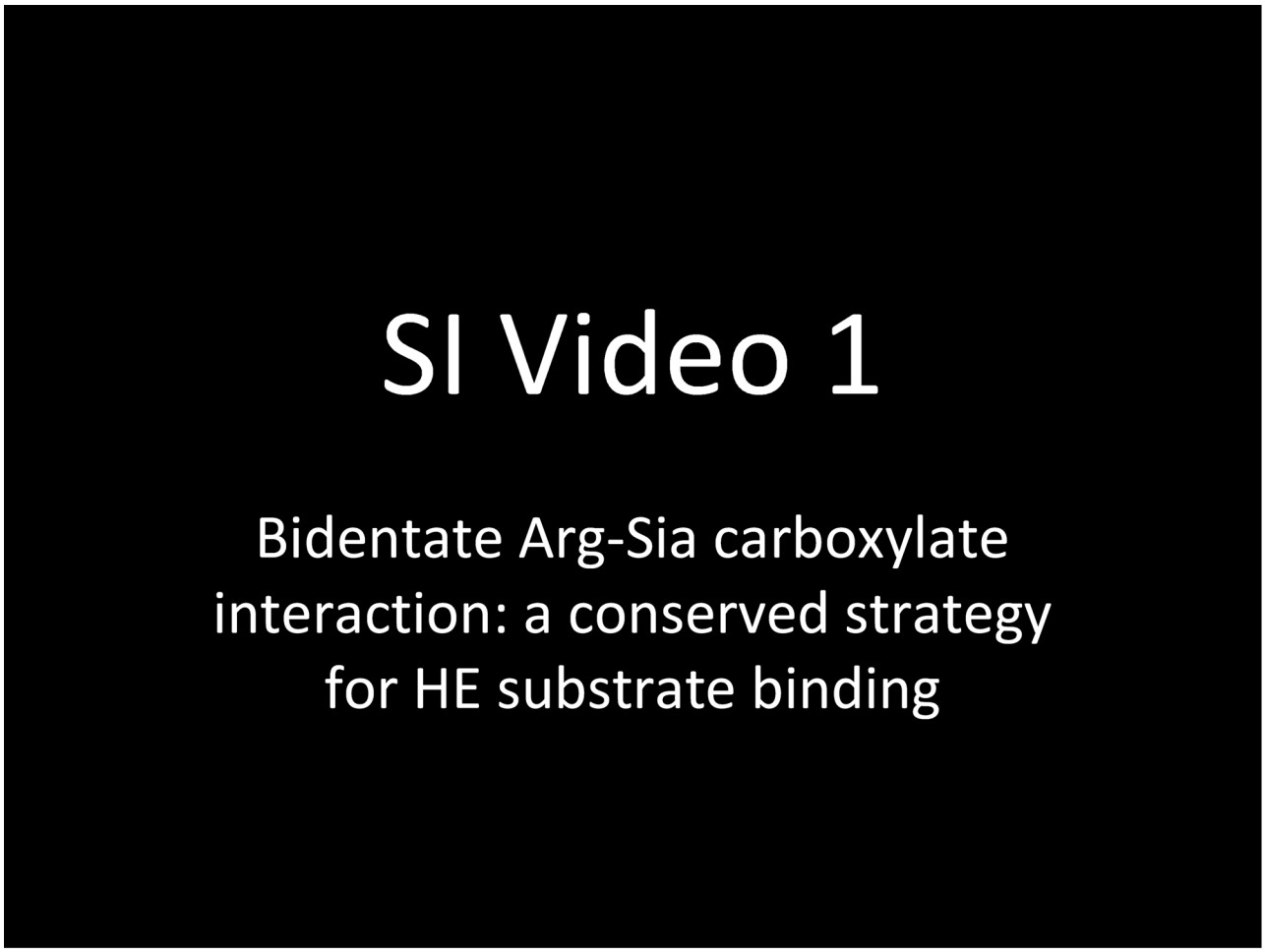

Movie S1. Bidentate arginine–sialic acid carboxylate interaction: a conserved strategy for HE substrate binding. Surface representation is shown of the PToV and BToV HE catalytic pockets. Substrate analog 9-*N*-acetyl sialic acid (Neu5,9*N*Ac$_2\alpha$2Me) modeled into the active site is shown in stick representation (carbon, cyan; nitrogen, blue; oxygen, red). The Sia-binding Arg residue (carbon, green) and the active-site residues composing the catalytic triad (carbon, magenta) and oxyanion hole (carbon, gray) are shown in stick representation. Note that in the model of BToV HE–substrate complex, Arg–Sia interaction is functionally, but not structurally conserved.

Movie S1 (WMV)

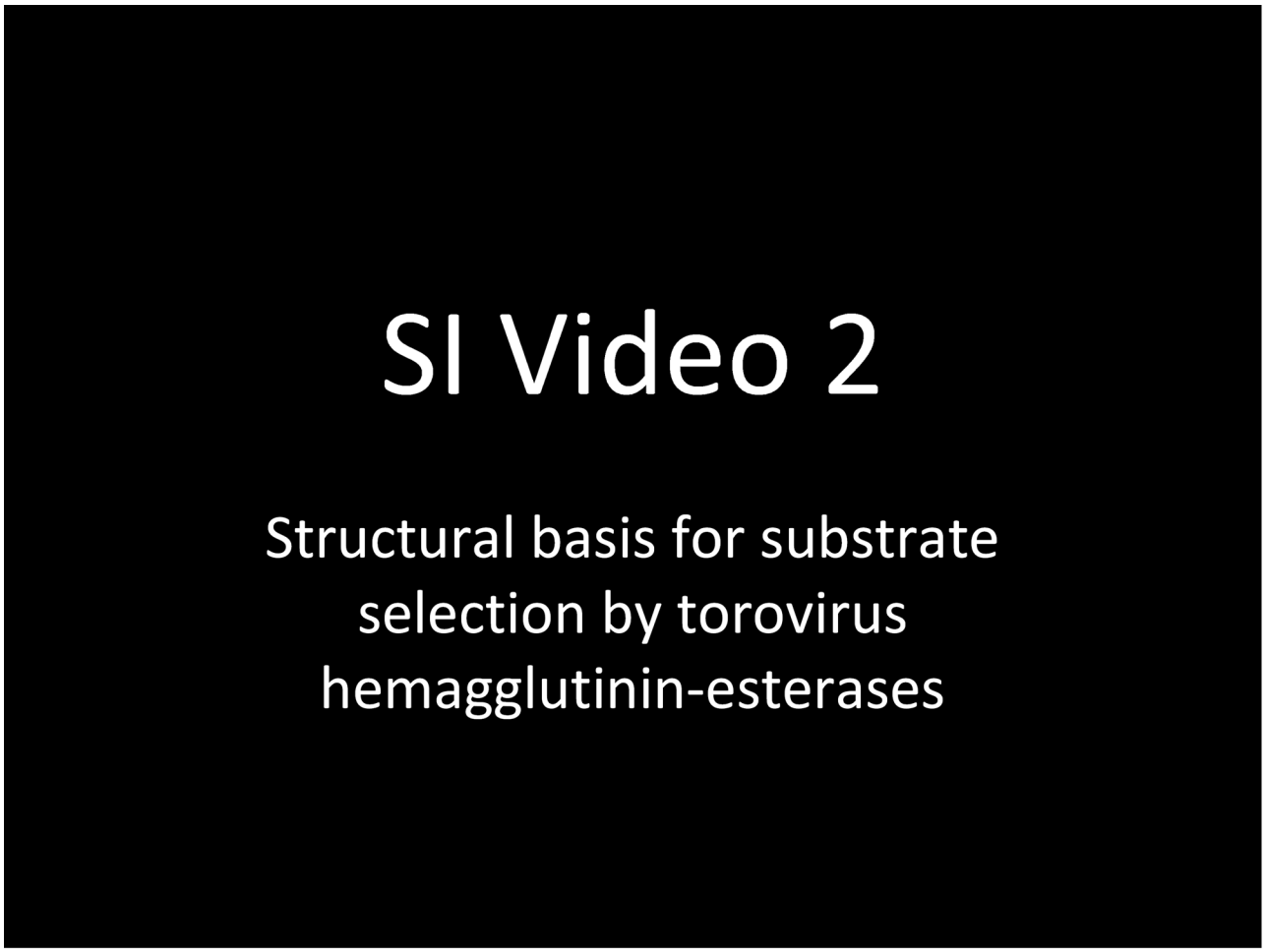

Movie S2. Structural basis for substrate selection by torovirus hemagglutinin esterases. A single-residue difference with BToV HE determines PToV HE preference for 9-mono- over 7,9-di-*O*-acetylated Sias. Surface representation is shown of the PToV and BToV HE active sites with surface patches contributed by Thr^{73} and Ser^{64} in the respective proteins colored in orange. Substrate analog 9-*N*-acetyl sialic acid (Neu5,9$NAc_2\alpha$2Me) modeled into the active site is shown in stick representation (carbon, cyan; nitrogen, blue; oxygen, red). For orientation, the Sia-binding Arg residue (carbon, gray) and the active-site residues composing the catalytic triad (carbon, magenta) and oxyanion hole (carbon, gray) are shown in stick representation. Note that the presence of Thr in PToV HE reduces the amount of free space available for substituents at the Sia C7 position.

Movie S2 (WMV)

Table S1. Structure and sequence similarity between different HEs

Domain	Item*	PToV and BToV HE	PToV and BCoV HE	BToV and BCoV HE	PToV HE and HEF	BToV HE and HEF	BCoV HE and HEF
Overall	Sequence identity (%)	67.7	33.2	32.4	35.5	33.6	29.5
	rmsd (Å)	0.87	1.56	1.81	1.64	1.77	1.82
	Aligned residues	353	319	321	318	327	315
MP	Sequence identity (%)	85.7	28.3	26.1	21.3	25.5	33.0
	rmsd (Å)	0.88	1.65	1.71	1.14	1.44	1.85
	Aligned residues	49	46	46	47	47	46
E	Sequence identity (%)	71.4	41.0	40.4	42.6	40.4	34.0
	rmsd (Å)	0.51	1.09	1.07	1.2	1.2	1.4
	Aligned residues	171	161	161	162	161	157
R	Sequence identity (%)	56.3	22.6	22.6	27.8	27.4	21.7
	rmsd (Å)	1.07	2.07	2.07	2.16	2.01	2.20
	Aligned residues	135	124	124	126	124	120

*Sequence identities and rmsd values were calculated for all residues whose Cα atoms superimpose within 5.0 Å.